at a perceptible rate. During the decay, the periodically taken cyclic voltammetric peaks gradually become shaped more like diffusional waves, and uncertainties in the coverage assay associated with this shape change make an adequately convincing inspection of the decay rate law difficult. Some useful insights can be gained simply from the time required for the apparent coverage of electroactive sites in the film to decrease to half the initial value. Such $t_{1/2}$ data are given in Table IIII.

The life data confirm[10d] that aging considerably increases the stability of plasma polymerized vinylferrocene films and also suggest that film stability varies with electrolyte. The data further show that only after weeks of aging do the plasma polymer films achieve the same stability as the preformed, photodeposited polymer, which has a half-life of 1-2 h. The aging effect may thus be less associated with a kinetics change for the chemistry by which ferrocenium sites are degraded than with a slow binding of low molecular weight oligomers in the plasma polymer to its cross-linked framework, avoiding loss of these units via leaching from the ferrocenium state film.

Acknowledgment. This research was supported in part by a grant from the National Science Foundation. This is publication 28 in a series on Chemically Modified Electrodes.

Registry No. Poly(vinylferrocene), 34801-99-5; Pt, 7440-06-4.

Contribution from the Max-Planck-Institut für Strahlenchemie,
D-4330 Mülheim a.d. Ruhr, Federal Republic of Germany

Photochemical Cleavage and Recombination Reactions of Matrix-Isolated (1-σ-4-6-η^3-Organo)tricarbonyliron Complexes

FRIEDRICH-WILHELM GREVELS* and WERNER E. KLOTZBÜCHER*

Received August 12, 1980

UV-visible irradiation of two isomeric (1-σ-4-6-η^3-organo)Fe(CO)$_3$ complexes, adducts of methyl acrylate and (η^4-dimethylbutadiene)tricarbonyliron, in inert and reactive matrices at 10-12 K was monitored by IR and UV spectroscopy. Detachment of CO is the only primary photoreaction. Subsequent reactions depend on the orientation of the ester group in the two isomers. Either the ester group is photoreversibly coordinated or the ejected CO is recaptured. Effective, stereospecific incorporation of a ligand from the matrix environment is observed for one of the isomers in experiments with ^{13}CO and N$_2$ matrices.

Introduction

Extended irradiation of pentacarbonyliron in the presence of olefin/1,3-diene mixtures results in coupling of the unsaturated substrates with formation of (1-σ-4-6-η^3-organo)tricarbonyliron complexes.[1,2] In particular, the substrate combination methyl acrylate/2,3-dimethylbutadiene yields two isomeric products, **1a** and **1b**,[1] which both are formed via either the (η^4-diene)Fe(CO)$_3$ or (η^2-olefin)Fe(CO)$_4$ complexes. More recently, (η^4-dimethylbutadiene)(η^2-methyl acrylate)dicarbonyliron (**2**) has been isolated as the key intermediate which reacts in the dark with carbon monoxide to form **1a** and **1b**.[3] Furthermore, **1a** and **1b** were shown[4] to undergo photochemical interconversion, **1a** ⇄ **1b**; concomitantly photocleavage leads back to (η^4-diene)Fe(CO)$_3$ and methyl acrylate, thus reducing the overall yield of **1**.

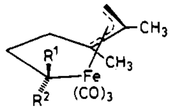

1a: R^1 = H, R^2 = CO$_2$CH$_3$
1b: R^1 = CO$_2$CH$_3$, R^2 = H

In order to obtain information about the intermediates involved in these reactions, we are investigating the photochemical behavior of the source materials and the products under low-temperature matrix-isolation conditions. A study with (η^4-diene)Fe(CO)$_3$ complexes has been reported previously.[5] In the present work we examine the photochemistry of the adducts **1a** and **1b** in inert and reactive matrices.

Experimental Section

Several details of the experimental equipment used in our photochemical and spectroscopic low-temperature investigations have been described previously.[5] An Air Products Displex closed-cycle helium cryostat was employed to cool a NaCl optical window to 10-12 K, the temperature being monitored by a thermocouple embedded in a drilled cavity close to the window center. The flow of matrix gas (99.99%, L'Air Liquide) was controlled by a calibrated micrometer needle valve and vacuum meter assembly, adjusted for each gas to a flow of approximately 2 mmol/h by a He-Ne laser interference fringe test.[6] The samples, purified and transferred under argon atmosphere, were deposited from a glass capillary held at constant temperature (32 °C for **1a**, 17 °C for **1b**) by a Peltier element, the temperature of which was separately monitored. In general a dilution of 1:1000 was attempted.

Infrared spectra were recorded on a Perkin-Elmer 580 instrument with the visible radiation (from the Nernst glower) removed by an Oriel CdTe filter. UV-visible spectra were taken with a Perkin-Elmer 356 two-wavelength spectrometer operating in the Split mode. For photochemical experiments the output of a Philips HPK 125 W high pressure mercury lamp was filtered through a 5-cm water cell to obtain "white" light with most of the infrared radiation removed. An air-cooled Schott GG 495 cutoff filter ($\lambda \gtrsim 495$ nm) replaced the cell for long-wavelength irradiations.

Results

The samples and their products were characterized by the CO stretching vibration patterns of the Fe(CO)$_n$ moieties and the CO stretching mode of the ester group in the infrared spectra and by the electronic absorptions in the UV-visible spectra. As the matrix-isolated compounds **1a** and **1b** behave somewhat differently in the irradiation experiments, they will be treated separately.

1. Irradiations of 1a. (a) In Inert-Gas Matrices. Figure 1A displays the characteristic Fe(CO)$_3$ pattern of **1a** isolated in argon at 10-12 K. The three strong absorptions appear in argon at 2068, 2012, and 1990 cm^{-1} and shift only slightly in different matrix materials (cf. Table I). In the ester carbonyl

---

(1) F.-W. Grevels, U. Feldhoff, J. Leitich, and C. Krüger, *J. Organomet. Chem.*, **118**, 79 (1976).

(2) F.-W. Grevels and I. Salama, to be submitted for publication.

(3) F.-W. Grevels and K. Schneider, *Angew. Chem.*, **93**, 417 (1981); *Angew. Chem., Int. Ed. Engl.*, **20**, 410 (1981).

(4) T. Akiyama and F.-W. Grevels, to be submitted for publication.

(5) G. Ellerhorst, W. Gerhartz, and F.-W. Grevels, *Inorg. Chem.*, **19**, 67 (1980).

(6) P. Groner, I. Stolkin, and Hs.H. Günthard, *J. Phys. E*, **6**, 122 (1973).

0020-1669/81/1320-3002$01.25/0

Table I. Infrared ($\tilde{\nu}$, cm^{-1}) and UV-Visible (λ, nm) Data of Complex **1a** and Its Photoproducts in Various Matrices at 10–12 K

	argon		krypton	xenon		N_2		^{12}CO		^{13}CO		hexane soln	
	IR	UV	IR	IR	UV	IR	UV	IR	UV	IR	UV	IR	UV
1a	2068	250	2064	2063		2066		2064		2064		2062.5	
	2012	340	2011	2006	345	2010	335	2007	335	2005	335	2006.5	340
	1990		1986	1985		1991		1988		1987		1984	
	1714		1712	1708		1711		1706		1707		1709	
3a	2025	305	2021	2019	310	2022	305	2020		2018			
	1971	485	1966	1965	510	1968	480	1964	485	1963	485		
	1715		1713	1709		(1711)		1705		(1707)			
4a	2013		2010	2006		2011		2006		2007			
	1955	440	1950	1948	440	1953	435	1950	450	1948	450		

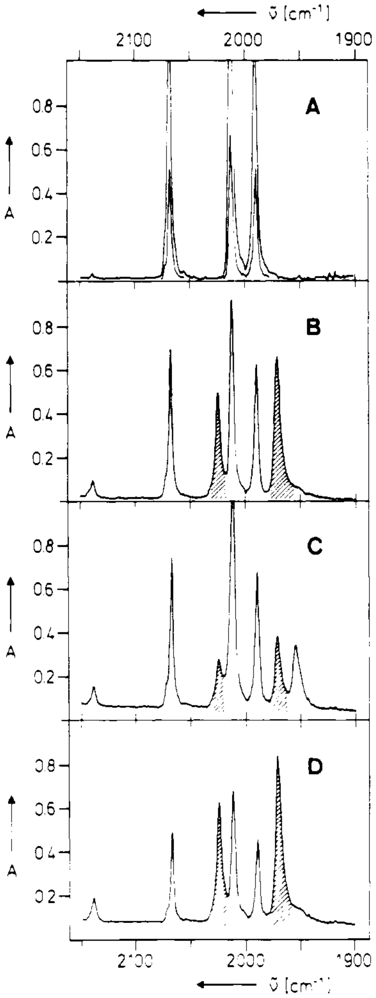

Figure 1. Infrared absorption spectra from experiments with complex **1a** in an argon matrix: (A) after 2.5- and 4.5-h deposition, respectively; (B) after subsequent 100 s of H_2O-filtered Hg arc irradiation; (C) after subsequent 60-min irradiation at λ ≳ 495 nm; (D) after further 120 s of H_2O-filtered Hg arc irradiation.

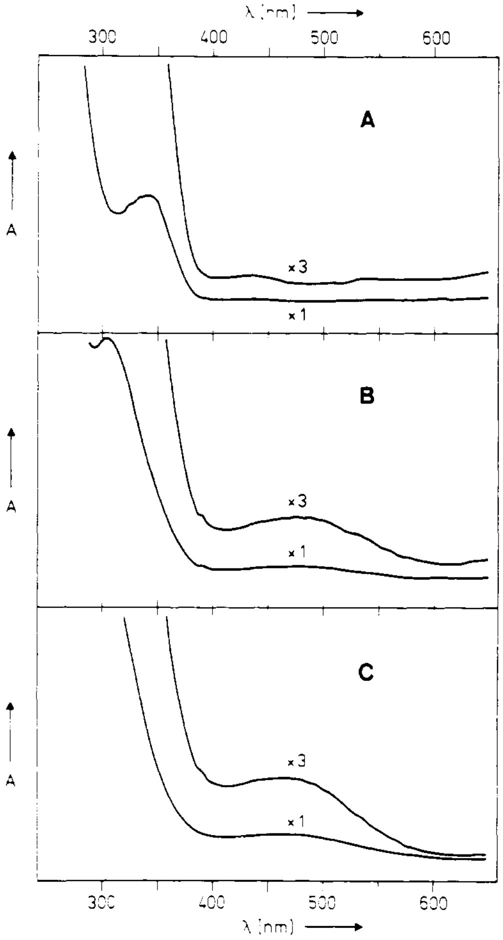

Figure 2. UV–visible absorption spectra from experiments with complex **1a** in an argon matrix; (A) after 4.5-h deposition; (B) after 100 s of H_2O-filtered Hg arc irradiation; (C) after 30-min irradiation at λ ≳ 495 nm.

region, a single absorption is observed in argon at 1714 cm^{-1}. The electronic absorption spectrum (Figure 2A) exhibits a distinct maximum at 340 nm on the tail of a very strong absorption centered at 255 nm.

Upon "white" irradiation the original three CO stretching bands of **1a** diminish, and two new bands grow in at 2025 and 1971 cm^{-1} together with a band at 2138 cm^{-1} associated with matrix-isolated "free" carbon monoxide (Figure 1B). Concomitantly the 340-nm absorption disappears while two new weak bands grow in, one at 305 nm and the other around 485 nm (Figure 2B). As the intensity ratio of the new bands in the infrared and UV–visible spectra remain constant throughout a series of irradiations, they are attributed to the same species, designated **3a**. Annealing to about 32 K (at which temperature bulk diffusion in argon matrices becomes significant) results in recovery, although to a minor extent, of **1a** at the expense of **3a**. Hence we conclude that the conversion **1a** $\xrightarrow{h\nu}$ **3a** involves merely the loss of one CO ligand whereas the organoiron complex skeleton is retained.

A similar recombination effect might be expected from long-wavelength irradiation, as demonstrated by studies with group 6 hexacarbonyls by Turner and co-workers.[7] And indeed one observes this effect upon irradiation of **3a** through the 495-nm cutoff filter, although this occurs only to a very small extent. At most 5% of **1a** can be recovered. The major reaction is a different one, resulting in the formation of a new species, **4a**, characterized by two infrared bands (Figure 1C) at 2012 and 1954 cm^{-1} (the first one overlapping with the

---

(7) J. K. Burdett, J. M. Grzybowski, R. N. Perutz, M. Poliakoff, J. J. Turner, and R. F. Turner, *Inorg. Chem.*, **17**, 147 (1978).

Scheme I

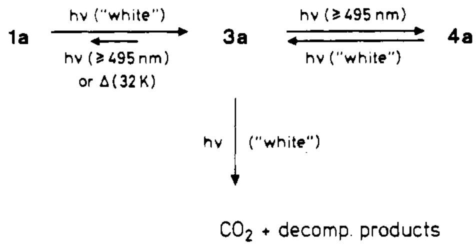

2012-cm^{-1} line of **1a**) and an electronic absorption at 440 nm (Figure 2C, showing the overlapping absorptions of **3a** and **4a**).

Upon subsequent "white" irradiation, **4a** rapidly (and quantitatively) converts back to **3a** which, under "white" irradiation conditions, remains the only product up to more than 90% conversion of the starting material **1a** (Figure 1D). Extensive further photolysis results in general decomposition into carbon dioxide (2343 cm^{-1}) and other, unidentified products.

Experiments in krypton and xenon matrices (cf. Table I) follow the pattern established above which can be summarized according to Scheme I.

(b) In Dinitrogen Matrices. Studies in N_2 matrices are of considerable interest as the matrix molecules sometimes can take possession of a coordination site at a metal complex fragment generated by photolysis. However, irradiations of **1a** in N_2 matrices did not yield dinitrogen complexes. The photolytic behavior (cf. Table I) was essentially the same as in inert-gas matrices, apart from a much larger recovery of **1a** from **3a** upon thermal annealing.

(c) In Carbon Monoxide Matrices. One intriguing question remains to be clarified, namely, whether the complexes under discussion can take up carbon monoxide from the matrix environment. "White" irradiation of **1a** in carbon monoxide matrices again results in formation of **3a** (cf. Table I). From here two directions can be explored. On stepwise warming up of the matrix to 34 K increasing and extensive recovery of **1a** on the order of 50% is observed. This occurs merely to a very minor extent upon long-wavelength irradiation ($\lambda \gtrsim$ 495 nm) where again the major product is **4a**. Actually, it is possible to go back and forth between **3a** and **4a** by consecutive long-and short-wavelength irradiations. Only upon very extensive "white" irradiation new lines (2050, 1984, 1970, 2026, 2002, and 1996 cm^{-1}) appear in the infrared spectrum which, as yet, we could not interpret reliably.

Experiments in pure ^{13}CO matrices (cf. Table I) give essentially the same results with no sign of ^{13}CO incorporation. Apparently carbon monoxide and dinitrogen matrices behave similarly but differ from inert-gas matrices in that the detached CO is kept close to the **3a** formed, thus facilitating recombination upon thermal annealing.

2. Irradiations of 1b. The infrared spectrum of complex **1b** (Figure 3A, Table II) resembles that of of the isomer **1a**, apart from red shifts in the order of 5–15 cm^{-1}. The UV–visible spectra of the two isomeric compounds are almost identical.

(a) In Argon Matrices. Similarly to the studies with **1a**, "white" irradiation of **1b** results in effective loss of carbon monoxide. The three lines of **1b** (cf. Table II) diminish in favor of the formation of a dicarbonyliron species characterized by CO stretching bands at 2021 and 1964 cm^{-1} and a well-resolved ester carbonyl absorption at 1704 cm^{-1}. These spectral changes parallel those associated with the conversion **1a** $\xrightarrow{h\nu}$ **3a**, as do the concomitant alterations in the UV–visible spectra, and consequently we designate the new species **3b**. Already at an early stage in these "white" irradiation experiments a second, minor product becomes apparent, characterized by a barely visible single line at 1943 cm^{-1} in Figure 3, suggesting the presence of a monocarbonyliron species.

Table II. Infrared ($\tilde{\nu}$, cm^{-1}) and UV-Visible (λ, nm) Data of Complex **1b** and Its Photoproducts in Various Matrices at 10–12 K

	argon		N_2		^{12}CO		^{13}CO		hexane soln	
	IR	UV	IR	UV	IR	UV	IR	UV	IR	UV
1b	2064	250	2063		2057		2060		2058	
	2005	340	2004	350	1996	320	2001	320	1999	340
	1986		1988		1981		1985		1981.5	
	1698		1696		1687		1690		1693	
3b	2021	300	2020		2011		2016			
	1964	485	1963	500	1953	480	1959	480		
	1704		1701		1693		1692			
4b	2013									
	1958	470								
5b			2220							
			2027	345						
			1978							
			1696							
1b′							2051			
							1996	320		
							1957			
3b′							2001			
							1925			

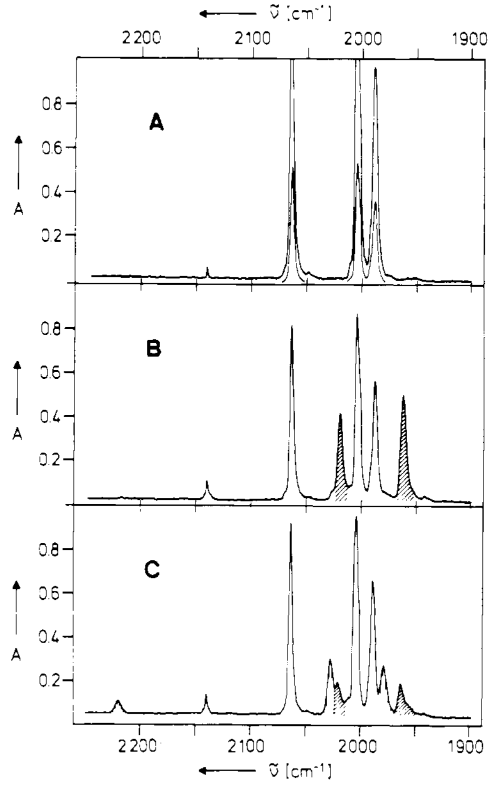

Figure 3. Infrared absorption spectra from experiments with complex **1b** in a dinitrogen matrix: (A) after 1.5- and 4-h deposition, respectively; (B) after 20 s of H_2O-filtered Hg arc irradiation; (C) after 30-min irradiation at $\lambda \gtrsim$ 495 nm.

In contrast to the behavior of **3a**, long-wavelength irradiation ($\lambda \gtrsim$ 495 nm) of the matrix containing **3b** results in considerable recovery of **1b** while the concomitant formation of a species **4b** (cf. Table II), the congener of **4a**, remains a minor process. Unfortunately, too little of **4b** is generated in this process to allow clear-cut identification with a weak broad band in the UV–visible spectrum centered at 470 nm. As in the studies with **1a**, extensive broad-band irradiation results in general decomposition.

(b) In Dinitrogen Matrices. Recall that in the case of **1a** dinitrogen acts like an inert-matrix material in that it is not incorporated into the photoproducts. As will be shown, the photochemistry of **1b** in dinitrogen (Figure 3) follows a different pattern. Upon long-wavelength irradiation of **3b**, generated as outlined before (Figure 3B), two reactions are observed, one being the recovery of a small amount of **1b**. The major reaction leads to the appearance of two new CO stretching bands at 2027 and 1978 cm^{-1}, *blue* shifted with regard to **3b**, together with a single line at 2220 cm^{-1}, characteristic of coordinated N_2[5,8] (Figure 3C). Hence, we attribute these new bands to (1-σ-4–6-η^3-organo)dicarbonyl(dinitrogen)iron (**5b**), a coordinately saturated complex in which the free coordination site of **3b** has been taken by a dinitrogen ligand. In support of this view, the position of the ester carbonyl band and the electronic absorption band (Table II) compare well with those of the parent compound **1b**. Incidentally, in consecutive short- and long-wavelength irradiations, it is possible to transform **5b** back to **3b**, and vice versa.

(c) In Carbon Monoxide Matrices. Again the dicarbonyliron species **3b** is formed upon "white" photolysis of **1b** in carbon monoxide (cf. Table II). Long-wavelength irradiation ($\lambda \gtrsim$ 495 nm) results in nearly complete recovery of **1b**; no trace of species **4b** can be detected. Thus, the trend already noticed for **3b** in argon prevails in carbon monoxide. Interestingly, decomposition upon extended "white" irradiation results in the appearance of only one tricarbonyliron pattern (2046, 1979, and 1965 cm^{-1}) which is similar to some of the bands observed upon photodecomposition of **1a** (see above). Simultaneously, spectral features at 2343 cm^{-1} (CO_2) and 1730–1733 cm^{-1} grow in gradually. The latter is probably associated with an α,β-unsaturated ester moiety. Apparently, the complex undergoes skeleton rearrangement and, possibly, hydrogen transfer in addition to decarboxylation of the ester group. However, in view of the scarce information available at present, we prefer not to speculate too much about these processes.

Concerning the effective recovery of **1b** upon long-wavelength irradiation of **3b**, we face the question whether the CO taken up originates from the CO previously detached from **1b** or from the matrix environment. The answer can be found in the analogous experiment in a pure-^{13}CO matrix (Figure 4). Long-wavelength irradiation of **3b** results in negligible recovery of **1b** while a new three-line pattern grows in (Figure 4C; cf. Table II), which is red-shifted with respect to **1b**. As far as the concomitant changes in the ester carbonyl region and in the UV–visible spectrum are concerned, there is essentially no difference between the experiments in ^{13}CO and ^{12}CO matrices. Hence, we are certain in our assignments of the new three-line pattern to a ^{13}CO-labeled **1b**, designated **1b′**. We have previously[3] shown that ^{13}CO-labeled **1b**, if prepared by reaction of **2** with ^{13}CO in solution, carries the label equally distributed over the three distinct CO positions and exhibits three well-resolved three-line CO stretching patterns (2055, 2054, 2046; 2001, 1994, 1986; 1971, 1955, 1947 cm^{-1} (in hexane)). Granted that some of the lines around 2050 and 1990 cm^{-1} could be hidden by overlapping bands under our experimental conditions, at least the lines around 1955 cm^{-1} should be clearly resolvable. The observation of only one line in this region unambiguously demonstrates that **1b′** carries the ^{13}CO label in one particular position.

Upon subsequent "white" irradiation, **1b′** diminishes together with some **1b** previously unreacted. In addition to the expected formation of **3b**, we observe two new lines growing in at 2001 and 1925 cm^{-1} (Figure 4D) which, with reference to the Teller–Redlich product rule,[9] are assigned to a ^{13}CO-labeled **3b**, designated **3b′**. Subsequent long- and short-wavelengths irradiations lead to further changes in the spectrum. However, the increasing number of overlapping bands impedes unequivocal intensity correlations. We thus prefer not to attempt assignments of the additional lines, especially as the incorporation of more than one ^{13}CO label could give rise to positional isomers.

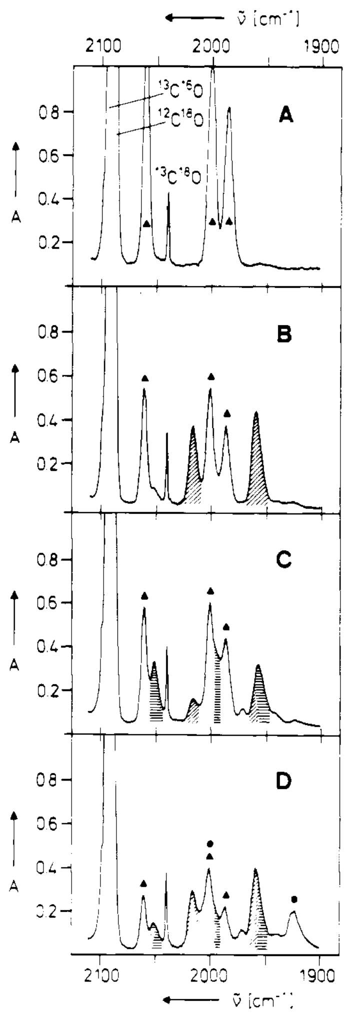

Figure 4. Infrared absorption spectra from experiments with complex **1b** in a ^{13}CO matrix: (A) after 6-h deposition; (B) after 40 s of H_2O-filtered Hg arc irradiation; (C) after 90-min irradiation at $\lambda \gtrsim$ 495 nm; (D) after further 60 s of H_2O-filtered Hg arc irradiation.

Discussion

Summarizing the results, we can, a priori, state that both of the (1-σ-4–6-η^3-organo)tricarbonyliron complexes, **1a** and **1b**, initially undergo photodetachment of one CO ligand. At first glance the infrared band positions of the resulting products **3a** and **3b** appear to be similar to those of **2** which had been shown to be a key intermediate in the photochemical synthesis of **1** in solution.[3] So that comparable infrared data could be obtained, the spectrum of **2** was recorded in solid argon. The number of lines (2028, 2023, 1983, 1973, 1730, 1715 cm^{-1}) reveals that matrix-isolated **2** exists as a mixture of isomeric species, as it does in solution.[3] The cited frequencies are sufficiently different from those of **3a** and **3b** to indicate that the latter two species are not identical with the isomeric components of **2**. Further support can be drawn from the fact that the characteristic long-wavelength absorption of **3a** and **3b** around 485 nm is absent in the UV–visible spectrum of **2**.

The most striking difference between **3a** and **3b** is the effective recovery of **1b** from the latter upon long-wavelength irradiation, whereas **3a** reforms the parent compound **1a** only to a minor extent but converts readily to another dicarbonyliron species (**4a**). As shown by the reactions in reactive matrices, **3b** alternatively recaptures the originally detached carbon

---

(8) W. Klotzbücher and G. A. Ozin, *J. Am. Chem. Soc.*, **97**, 2672 (1975).

(9) P. S. Braterman, "Metal Carbonyl Spectra", Academic Press, London, 1975.

Scheme II

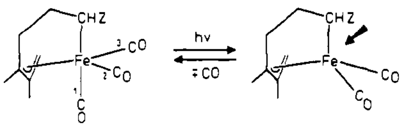

monoxide or takes up a ligand from the matrix environment. It is quite evident from the observation of only *one* N_2-substituted and only *one* ^{13}CO-labeled product (**5a** and **1b**′, respectively) that the entering ligand is not randomly distributed but rather introduced stereospecifically. On the other hand, photolytic detachment of CO from **1b** occurs, at least in part, not from this particular position, as witnessed by the loss of unlabeled CO from **1b**′, yielding ^{13}CO labeled **3b**′ upon "white" irradiation.

Bearing in mind that **3a** does not take up a ligand from the matrix environment, we can suspect that in this case the entering position is effectively shielded. Most likely this is due to the ester group, the position of which is the only significant difference between the two isomers. Intuitively one might expect that after detachment of one CO (regardless of which) from **1** the remaining two CO ligands of **3** will slightly rearrange to occupy positions of least sterical hindrance, as depicted in Scheme II. A ligand attack from below would not be hindered by the ester group regardless of its position and consequently could not explain the different behavior of **3a** and **3b**. We therefore have to assume that the ligand enters from above. Figure 5 presents a view of the situation along the Fe–C σ bond with the ester groups oriented as in the parent tricarbonyliron complexes.[1,10] Immediately one recognizes the shielding function of the ester group in **3a** and the most probable direction of ligand attack at **3b** as indicated by the arrow. Consequently the label in **1b**′ and the N_2 ligand in **5b** should occupy position 2 of the parent molecule **1b** (cf. Scheme II).

It remains to discuss the identity of **4a** (cf. Scheme I). The red shift of the CO stretching frequencies indicates increased metal → π^*(CO) back-donation. It is quite likely that the ester group fills the vacant coordination site, thus acting as a donor ligand which should increase the electron density at the metal. Unfortunately, the ester carbonyl stretching vibration of **4a** could not be located, precluding a more certain identification of this species. However, in agreement with our proposal, the low-energy electronic absorption of the coordinately unsaturated **3a** is shifted to a higher frequency position which could be due to the stabilization of an occupied metal orbital by interaction with the ester carbonyl group.

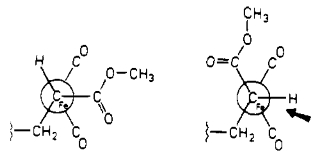

Figure 5. View along the Fe–C σ bond of complexes **1a**/**3a** and **1b**/**3b**, showing the differing positions of the ester group. The η^3-allyl moiety is omitted for clarity.

Detailed knowledge of the electronic structure of complexes **1** is still missing at present. It has been pointed out[5,11] that for (η^4-diene)Fe(CO)$_3$ complexes a variety of different excited states can be expected, some of which are only slightly separated in energy, involving both the organic and the CO ligands. This should hold true even more for the less symmetrical complexes **1**.

There is no indication of an isomerization from the "**a**" to the "**b**" series (and vice versa) at any stage of the irradiations in low-temperature matrices. Therefore, we assume that the photoisomerization **1a** ⇄ **1b** observed in solution does not occur directly from an electronically excited state but rather results from *thermal* rearrangement subsequent to the initial photolytic detachment of CO. On the other hand, secondary photochemical steps could be involved in the photolytic C–C bond cleavage (leading back to (η^4-diene)Fe(CO)$_3$ and methyl acrylate) and in other solution photoreactions[1,2,4] of **1a** and **1b**.

Acknowledgment. This work was supported by the Deutsche Forschungsgemeinschaft. We are indebted to Dr. W. Gerhartz for performing some preliminary experiments. Assistance by K. Schneider and G. Deege is gratefully appreciated.

Registry No. **1a**, 61950-05-8; **1b**, 61867-50-3; **3a**, 77744-92-4; **3b**, 77841-53-3; **4a**, 77744-93-5; **4b**, 77841-54-4; **5b**, 77744-94-6.

---

(10) A.-P. Chiang and C. Krüger, to be submitted for publication.

(11) F. Mark and H. Weigel, to be submitted for publication; H. Weigel, Diplomarbeit, Universität Dortmund.